Dalton Transactions

PAPER

View Article Online
View Journal | View Issue

Cite this: *Dalton Trans.*, 2014, **43**, 13041

Copper(II) complexes of bis(aryl-imino)-acenaphthene ligands: synthesis, structure, DFT studies and evaluation in reverse ATRP of styrene†

Christophe Fliedel,[a] Vitor Rosa,[a] Carla I. M. Santos,[a] Pablo J. Gonzalez,[a] Rui M. Almeida,[a] Clara S. B. Gomes,[b] Pedro T. Gomes,*[b] M. Amélia N. D. A. Lemos,[c] Gabriel Aullón,*[d] Richard Welter[e] and Teresa Avilés*[a]

Two new Ar-BIAN Cu(II) complexes (where Ar-BIAN = bis(aryl-imino)acenaphthene) of formulations [$CuCl_2$(Mes-BIAN)] (**1**) (Mes = 2,4,6-$Me_3C_6H_2$) and [$CuCl_2$(Dipp-BIAN)] (**2**) (Dipp = 2,6-$iPr_2C_6H_3$) were synthesised by direct reaction of $CuCl_2$ suspended in dichloromethane with the respective ligands Mes-BIAN (**L1**) and Dipp-BIAN (**L2**), dissolved in dichloromethane, under an argon atmosphere. Attempts to obtain these compounds by solubilising $CuCl_2$ in methanol and adding a dichloromethane solution of the corresponding ligand, under aerobic conditions, gave also compound **1**, but, in the case of **L2**, the Cu(I) dimer [CuCl(Dipp-BIAN)]$_2$ (**3**) was obtained instead of compound **2**. The compounds were fully characterised by elemental analyses, MALDI-TOF mass spectrometry, FT-IR, ^{1}H NMR and EPR spectroscopic techniques. The solid-state molecular structures of compounds **1–3** were determined by single crystal X-ray diffraction, showing the expected chelation of the Ar-BIAN ligands and two chloride ligands completing the coordination sphere of the Cu(II) centre. In the case of the complex **1**, an intermediate coordination geometry around the Cu(II) centre, between square planar and tetrahedral, was revealed, while the complex **2** showed an almost square planar geometry. The structural differences and evaluation of energetic changes were rationalised by DFT calculations. Analysis of the electrochemical behaviour of complexes **1–3** was performed by cyclic voltammetry and the experimental redox potentials for Cu(II)/Cu(I) pairs have been compared with theoretical values calculated by DFT in the gas phase and in dichloromethane and methanol solutions. The complex **1** exhibited good activity in the reverse atom transfer radical polymerisation (ATRP) of styrene.

Received 10th April 2014,
Accepted 20th June 2014

DOI: 10.1039/c4dt01069h

www.rsc.org/dalton

Introduction

The design and synthesis of copper complexes is a subject of current interest since they can be applied in a large variety of metal-mediated transformations.[1,2] One of the most important applications is the Cu-mediated controlled/"living" radical polymerisation. This type of polymerisation was independently reported in 1995 by Matyjaszewski[3] and Sawamoto,[4] and has, since then, been the subject of many publications and reviews.[5–9] Atom transfer radical polymerisation (ATRP) is successfully mediated by a variety of transition metals, however the copper complexes have been found to be the most versatile and convenient catalytic systems for this process because of the low cost of the copper source, their efficiency and the possibility to fine-tune the stereo-electronic properties of the copper complexes with a variety of suitable ligands.[10–12] The process can be started from Cu^I complexes, often air- and moisture-sensitive, together with a halogenated compound (R–X) as an initiator, in the presence of a monomer (so-called

[a]*REQUIMTE, Departamento de Química, Faculdade de Ciências e Tecnologia, Universidade Nova de Lisboa, Caparica, 2829-516, Portugal. E-mail: teresa.aviles@fct.unl.pt*
[b]*Centro de Química Estrutural, Departamento de Engenharia Química, Instituto Superior Técnico, Universidade de Lisboa, Av. Rovisco Pais, 1049-001 Lisboa, Portugal. E-mail: pedro.t.gomes@tecnico.ulisboa.pt*
[c]*IBB/CERENA, Instituto Superior Técnico, Universidade de Lisboa, Av. Rovisco Pais, 1049-001 Lisboa, Portugal*
[d]*Departament de Química Inorgànica and Institut de Química Teòrica i Computacional, Av. Diagonal 645, 08028 Barcelona, Spain. E-mail: gabriel.aullon@qi.ub.es*
[e]*Institute of Plant Molecular Biology of CNRS UPR 2357, University of Strasbourg, F-67084 Strasbourg, France*

†Electronic supplementary information (ESI) available: Figures containing the mass spectra of compounds **1–3** and the corresponding simulations (Fig. S1–S4), the ^{1}H NMR spectra of complexes **1** and **2** (Fig. S5), the cyclic voltammograms of complexes **1**, **2** and **3** (Fig. S6 and S7), and ^{1}H and $^{13}C\{^1H\}$ NMR spectra of a polystyrene sample (Fig. S8–S10); tables containing polymerisation reaction data and the corresponding polystyrene molar masses (Table S1), and coordinates for optimised geometries of Cu species (Table S2). CCDC 994399–994401. For ESI and crystallographic data in CIF or other electronic format see DOI: 10.1039/c4dt01069h

ATRP conditions) or, on the other hand, it can be started from a stable Cu^{II} complex and a standard radical source, in the presence of a monomer (so-called reverse ATRP conditions).

α-Diimine ligands have been known since the late 1960s[13,14] and have been extensively used due to their ability to stabilise organometallic complexes.[15] More recently, Elsevier *et al.*[16] described the synthesis and full characterisation of rigid chelating bidentate ligands of the type Ar-BIAN (bis(arylimino)acenaphthene) by condensation of the acenaphthenquinone with 2 equiv. of an appropriate aryl-amine. Using these synthetic routes, we can easily vary the backbone and the aryl substituent, enabling thus the modification of the steric and electronic effects at the metal centre. A large number of late transition metal complexes bearing α-diimine ligands have been extensively employed in several catalytic reactions.[17–22] We have been engaged for the past few years in the synthesis of α-diimine transition metal compounds.[23,24] It is noteworthy that Ar-BIAN ligands allowed the stabilisation of zinc(II) cationic alkyl complexes, highly active in the ring-opening polymerisation (ROP) of ε-caprolactone.[25] Furthermore, copper(I)[26] and copper(II)[27] complexes, bearing Ar-BIAN ligands, have been reported by us and other authors; for instance Ar-BIAN-based copper(I) complexes were shown to be active catalysts for the copper(I)-catalysed azide–alkyne cycloaddition reaction (CuAAC).[28]

Herein, we describe the synthesis and full characterisation of [$CuCl_2$(Ar-BIAN)] complexes, where Ar = 2,4,6-$Me_3C_6H_2$ (**1**) and 2,6-$iPr_2C_6H_3$ (**2**), and rationalise their different reactivities in the light of electrochemical and density functional theory (DFT) studies. The combination of the neutral supporting bidentate nitrogen ligand and halides (Cl) in the coordination sphere of copper, as well as the facile change in the oxidation state at the copper centre without decomposition, prompted us to study the complexes [$CuCl_2$(Ar-BIAN)] as catalysts for the reverse ATRP of styrene.

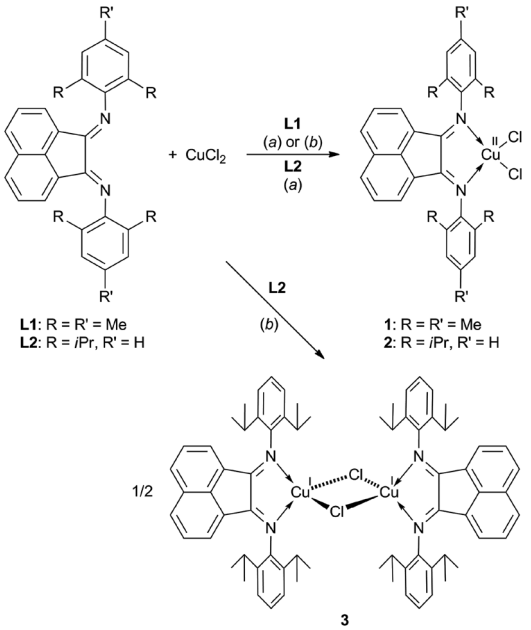

Scheme 1 Synthesis of Cu(II) complexes **1** and **2** and the Cu(I) complex **3**. Method (*a*): under an Ar atmosphere, **L1** or **L2** (1 equiv.), $CuCl_2$ (1 equiv.), CH_2Cl_2, room temp., 12 h. Method (*b*): in air, **L1** or **L2** (1 equiv.), $CuCl_2$ (1 equiv.), CH_2Cl_2–MeOH, room temp., 2 h.

Results and discussion

(a) Synthesis and characterisation

The ligands Mes-BIAN (**L1**) (Mes = 2,4,6-$Me_3C_6H_2$) and Dipp-BIAN (**L2**) (Dipp = 2,6-$iPr_2C_6H_3$) were prepared as previously reported.[16] The Cu(II) complexes [$CuCl_2$(Mes-BIAN)] (**1**) and [$CuCl_2$(Dipp-BIAN)] (**2**) could be obtained in good yields (about 90%) by treatment of a dichloromethane suspension of $CuCl_2$ with a solution of the appropriate ligand in the same solvent, at room temperature, under an inert atmosphere (Scheme 1, method (*a*)). Complexes **1** and **2** were obtained as intense coloured brown and green crystals, respectively, being moderately soluble in chlorinated solvents and insoluble in Et_2O or pentane. Suitable crystals for X-ray diffraction studies were obtained by slow diffusion of diethyl ether or pentane into saturated dichloromethane solutions of **1** and **2**, respectively. The compounds have been fully characterised by elemental analyses, MALDI-TOF-MS, FT-IR, ^{1}H NMR and EPR spectroscopic techniques and single-crystal X-ray diffraction studies. The expected structures of complexes **1** and **2** were confirmed by X-ray crystallographic studies, and are discussed in the X-ray diffraction subsection.

When the reaction was performed under aerobic conditions, using methanol as the solvent to solubilise the copper(II) precursor, different behaviours for the two reactions were observed. While the reaction of a methanol solution of $CuCl_2$ (5 mL) with a dichloromethane solution of **L1** (15 mL) gave the complex **1**, stable in air, in similar yield to those described above (Scheme 1, **L1** method (*b*)), the reaction with a dichloromethane solution of **L2** (15 mL) proceeded in a completely different route (Scheme 1, **L2** method (*b*)). In the first stage, green crystals were formed (presumably of the complex **2**), which were left in the reaction mixture and, after 48 hours, black crystals were isolated in nearly 45% yield. Single crystal X-ray diffraction studies performed on the latter crystals revealed the formation of the Cu(I) dimer [CuCl(Dipp-BIAN)]$_2$ (**3**), the product of a reduction process. This reduction reaction, occurring under aerobic conditions, is likely due to methanol acting as a reducing agent. In fact, Cu(II) complexes have been extensively used in the catalytic aerobic oxidation of alcohols.[29] The structure of compound **3** is isomorphic to those recently reported by us[28b] and other authors,[30] which were obtained by different routes, namely by treatment of CuCl, a Cu(I) precursor, with **L2**. Attempts to rationalise the factors responsible for the structural differences between complexes **1** and **2**, as well as their different behaviour in the presence of MeOH under aerobic conditions, *i.e.* reduction of **2** to the Cu(I) dimer **3**, led us to perform electrochemical studies

Table 1 Molar magnetic susceptibilities and the number of unpaired electrons of complexes **1** and **2**, obtained by the Evans method

Complex	Mass[a] (mg)	TMS shift[b] (Hz)	χ[c] (m^3 mol^{-1})	Number of unpaired electrons[d] (calc.)
1	6.0	59.87	1.86×10^{-3}	1.3
2	8.5	30.27	0.98×10^{-3}	0.9

[a] The mass of the compound (mg) dissolved in 500 μL CD_2Cl_2. [b] The TMS frequency shift in a 9.4 T magnetic field (Hz). [c] Molar magnetic susceptibility (χ) (m^3 mol^{-1}). [d] The calculated number of unpaired electrons.

and DFT calculations, in order to compare them with the experimental results (see subsections below).

Experimental and simulated MALDI-TOF mass spectra can be found in ESI (Fig. S1–S4†). For both complexes **1** and **2**, the molecular ion peaks are absent, but the fragments $[M - Cl]^+$, m/z = 514.11 (**1**) and m/z = 598.19 (**2**) were found, their isotopic pattern being in perfect agreement with the corresponding simulated spectra. The major peak present in the spectrum of the complex **1** corresponds to the ligand fragment $[\mathbf{L1} - CH_3]^+$ (m/z = 401.21). This fragmentation is quite uncommon for this ligand and was also found in the complex **2** with the loss of an iPr group, resulting in the presence of the $[\mathbf{L2} - iPr]^+$ (m/z = 457.24) fragment. For the complex **3**, the molecular ion was also absent, the fragment $[M - Cl]^+$, m/z = 1161.39 being found and fitting well with the simulated one.

The FT-IR spectra of complexes **1** and **2** showed absorption bands at ν = 1660, 1638 cm^{-1} (**1**) and ν = 1666, 1636 cm^{-1} (**2**), attributed to the (C═N) vibrations. In the Far-IR region, absorption bands at ν = 524, 357, 323 cm^{-1} for **1** and ν = 526, 355, 321 cm^{-1} for **2** attributed to the Cu–Cl vibrations were observed.

The ^1H NMR spectra of Cu(II) complexes **1** and **2** show broad resonances between 10 and 18 ppm (see Fig. S5 in ESI†), which are due to the paramagnetism of both compounds. Molar magnetic susceptibility measurements were carried out by the Evans method (see the Experimental section), leading to the expected number of unpaired electrons for these Cu(II) complexes (Table 1).

(b) EPR spectroscopy

The EPR spectra of polycrystalline samples of **1** and **2** (Fig. 1A and C, respectively) as well as those of a frozen CH_2Cl_2 solution of **1** (Fig. 1B) were recorded. No significant differences were observed in the line shapes of the powdered samples in the range 4–298 K.

The EPR spectrum of polycrystalline powder of **1** shows a quasi-axial symmetry (Table 2 and Fig. 1A). The EPR parameters observed in the powder sample are different from those observed in the frozen CH_2Cl_2 solution (Table 2). The EPR spectrum of the frozen solution of **1** (Fig. 1B) also shows a nearly-axial symmetry but with $g_{\|} > g_{\perp}$. The g-values predicted through DFT calculations, in which the crystal packing is not present but the tetrahedral distortion was taken into account, also yielded $g_{\|} > g_{\perp}$. This might indicate that the g-values

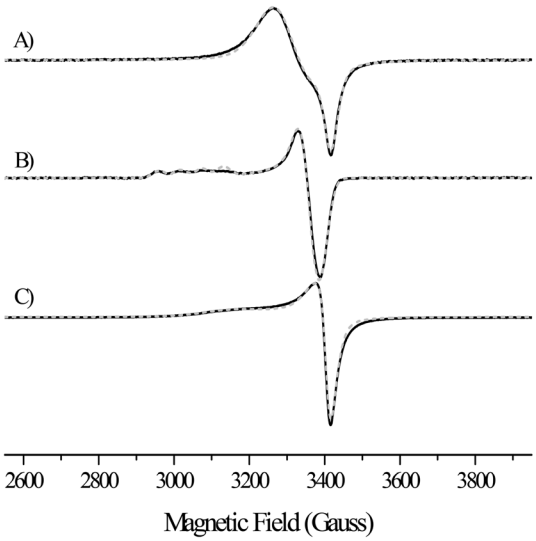

Fig. 1 EPR spectra of polycrystalline samples of **1** (A) and **2** (C), and frozen CH_2Cl_2 solution of **1** (B). Experimental spectra are plotted as black lines and simulations are overlaid as grey dashed lines.

Table 2 Computational and experimental EPR parameters obtained from computer simulation of experimental data using Simfonia v.1.25. Values between parentheses are the linewidths in Gauss. The shape parameter Lorentzian/Gaussian for powder samples and the CH_2Cl_2 solution were 0.1 and 1, respectively. The g-values obtained from DFT calculations are also reported for comparison

		g_1	g_2	g_3	A_1 (Gauss)
1	Powder	2.130 (120)	2.125 (90)	2.051 (30)	—
	Solution	2.265 (35)	2.059 (40)	2.037 (40)	57
	DFT	2.134	2.043	2.042	—
2	Powder	2.225 (150)	2.059 (55)	2.053 (20)	—
	DFT	2.126	2.041	2.040	—

observed in the polycrystalline powder are the average of non-equivalent copper ions resulting from exchange interactions between monomers within the crystal.

On the other hand, the experimental EPR spectrum of a polycrystalline powder of **2** as well as the one predicted through DFT calculations show nearly-axial symmetry with $g_{\|} > g_{\perp}$, which is usually observed in Cu(II) ions having a tetra-coordinated planar geometry, and is therefore consistent with the square-planar geometry around the Cu(II) centre revealed in the solid-state structure of **2** (see below). The hyperfine structure produced by the Cu(II) nucleus (I = 3/2) was not observed in the powder samples presumably because it is collapsed by exchange interactions between Cu(II) ions from neighbouring monomers.

(c) X-ray diffraction

The expected structures of both dichloride copper complexes **1** and **2** could be unambiguously confirmed by single crystal X-ray diffraction analyses (Fig. 2). The structures reveal a distorted square planar coordination geometry around the copper centre in **1** (Fig. 2A), while that of **2** is closer to square-

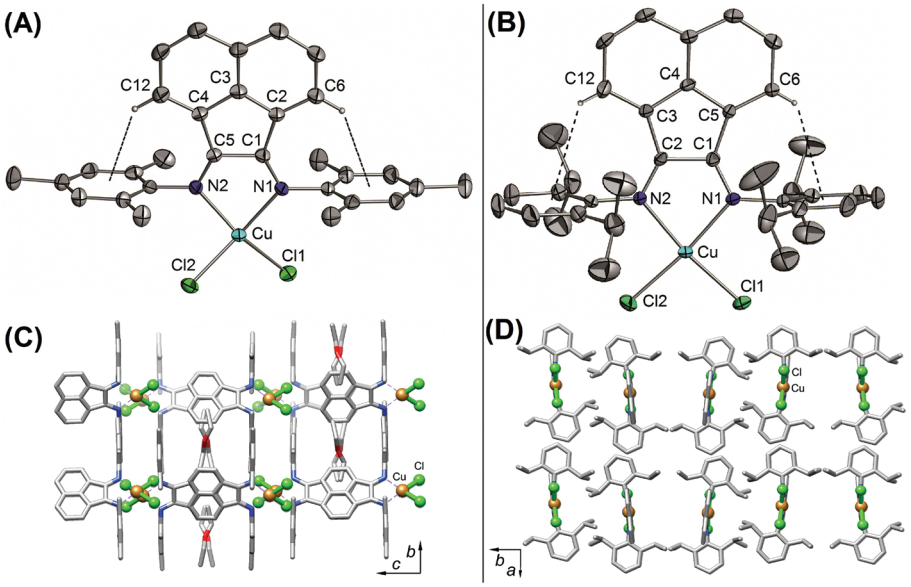

Fig. 2 Views of the molecular structures of **1**·OEt_2 (A) and **2**·CH_2Cl_2 (B) and their respective packings (C) and (D). Hydrogen atoms and solvent molecules omitted for clarity. Selected bond lengths (Å) and angles (°) for (**1**·OEt_2): Cu–N1 2.047(4); Cu–N2 2.049(4); Cu–Cl1 2.2001(13); Cu–Cl2 2.1997(13); C1–N1 1.281(6); C5–N2 1.272(6); Cl1–Cu–Cl2 96.36(5); N1–Cu–N2 81.26(15); and for (**2**·CH_2Cl_2): Cu–N1 2.045(2); Cu–N2 2.058(2); Cu–Cl1 2.2051(10); Cu–Cl2 2.1961(11); C1–N1 1.287(4); C2–N2 1.285(4); Cl1–Cu–Cl2 95.67(4); N1–Cu–N2 81.14(9).

planarity (Fig. 2B). These structural differences could be illustrated by views along the *a*- and *c*-axes of the molecular packing of **1**·OEt_2 and **2**·CH_2Cl_2, respectively (Fig. 2C and D).

The deviation angle of the regular square planar geometry could be obtained by measuring the angle between the N1–Cu–N2 and Cl1–Cu–Cl2 planes, which was found to be 23.67° for **1** and 1.54° for **2**. This fact was initially attributed to the bulkier *ortho*-substituents on the *N*-aryl groups of ligand **L2** compared to **L1**. We can observe that no significant intra- or intermolecular interaction can rationalise this structural difference (Fig. 2C and D). The representative C=N, N–Cu and Cu–Cl bond lengths of complexes **1** and **2** are in the range of those found in other tetracoordinated bis-imine dichloride copper complexes (1.28 < C=N < 1.40; 1.97 < N–Cu < 2.06; 2.19 < Cu–Cl < 2.25).[31,32] A more detailed structural analysis of these examples, composed of square planar[32] and tetrahedral distorted[31] [(N–Cu–N)–(Cl–Cu–Cl) angle = 46–65°] geometries, does not confirm our initial guess. In fact, within these examples, some of them contain *N*-aryl groups with bulky *ortho*-substituents and exhibit a distorted geometry and *vice versa*. To obtain a better insight, the steric and/or the electronic contribution of the ligands to the Cu coordination geometry in **1** and **2**, theoretical investigations were performed (see below). The solid-state structure of complexes **1** and **2** illustrate the good steric protection provided by the *N*-aryl BIAN ligands, preventing the formation of dimeric structures, by the chloro-bridged ligand, as often seen in the literature.[33] The protection of the copper centre could be a key point for the stabilisation of the catalytically active Cu(I) radical species in the reverse ATRP reaction.

Attempts to obtain **2** by the synthetic method B under aerobic conditions led to the formation of black crystals of a

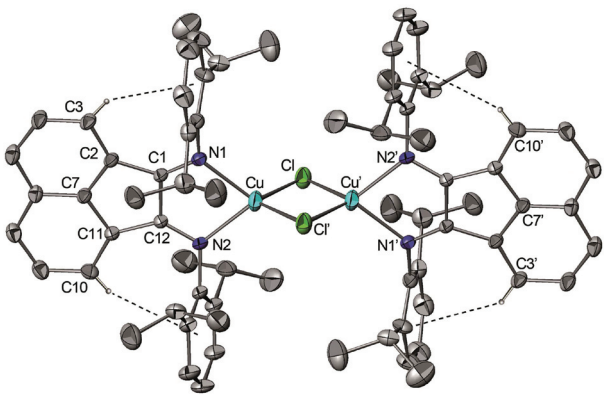

Fig. 3 View of the molecular structure of **3**. Hydrogen atoms omitted for clarity. Selected bond lengths (Å) and angles (°): Cu–N1 2.088(2); Cu–N2 2.091(2); Cu–Cl 2.2752(11); Cu–Cl′ 2.2935(8); C1–N1 1.288(3); C12–N2 1.287(3); Cl–Cu–Cl′ 105.90(4); N1–Cu–N2 81.15(10).

centrosymmetric chloro-bridged copper(I) dimer **3**. Halide-bridged copper(I) dimers can also be synthesised by direct and stoichiometric reaction of the respective copper(I) salt with the Ar-BIAN ligand.[28b,30] The molecular structure of **3** (Fig. 3) reveals a slightly distorted tetrahedral coordination geometry around the metal. The bite angle of the ligand (N1–Cu–N2) lies in the classical range of values (~81°) and the angle between the planes (N1–Cu–N2)–(Cl1–Cu–Cl1′) of 84.1° is close to the expected 90°. The Cu–Cl bonds in the complex **3** are slightly longer than in the case of the monomeric structures of **1** and **2**, due to the shared electronic density between the two copper centres. The reduction of the copper centre from +2 to +1, instead of the presence of a delocalized electron in a

Table 3 Reduction peak potentials measured for complexes **1** and **2** in CH_2Cl_2 and MeOH. All potentials given in volts *vs.* Fc^+/Fc redox couple and *vs.* SHE

	vs. Fc^+/Fc (internal standard)			*vs.* SHE		
	CH_2Cl_2		MeOH	CH_2Cl_2		MeOH
Complex	E_p^{red} (I)	E_p^{red} (II)	E_p^{red} ($E_{1/2}^{red}$)	E_p^{red} (I)	E_p^{red} (II)	E_p^{red} ($E_{1/2}^{red}$)
1	−0.26	−1.98	−0.05 (0.05)	0.49	−1.24	0.59 (0.69)
2	−0.30	−1.99	−0.04 (0.06)	0.44	−1.25	0.61 (0.70)

"charged" BIAN ligand, is verified by the diamagnetic nature of the complex **3** (see the Experimental section), and classical bond lengths and angles within the ligand and between the ligand and the metal for a bis-imine copper(I) chloride complex.[30,34] These facts, as well as the relative inertia of the complex **1** compared to **2** towards air-mediated reduction of copper(II) to (I), can be rationalised by the electron density calculations performed on these systems (see below).

(d) Electrochemistry

We have recently reported the electrochemical behaviour of a series of copper(I) complexes similar to the ones presented in this study.[28a] In particular, the mono-chelated complexes of the type $[Cu(Ar\text{-}BIAN)L_2]BF_4$ (where Ar = 2,6-$iPr_2C_6H_3$, L = NCPh or NCMe) featured two redox processes, a partially reversible oxidation and an irreversible reduction, which were assigned to the Cu(II)/Cu(I) and Cu(I)/Cu(0) redox couples, respectively. Herein, the copper complexes in the oxidation state +2, bearing Ar-BIAN ligands and two chlorides (**1** and **2**), were studied in two different solvents, CH_2Cl_2 and MeOH, in order to gain a better insight into the different reactivities observed for complexes **1** and **2**, and the formation of **3** (see the Synthesis and characterisation section). The electrochemical behaviour now reported for **1** and **2**, in CH_2Cl_2, bears similarities to the above mentioned complexes. Both compounds undergo a reduction process that is irreversible in all the scan rates studied (from 50 mV s^{-1} up to 800 mV s^{-1}), occurring at a peak potential of 0.49 V and 0.44 V *vs.* SHE for **1** and **2** (Fig. S6a in ESI†), respectively, as shown in Table 3 and exemplified in Fig. 4 for **2**, in agreement with a Cu(II) → Cu(I) reduction process.

A further reduction wave is observed at a much lower potential (around −1.2 V for both **1** and **2**). However, it falls in the limits of the potential window available with this electrolyte solution ($[NBu_4][BF_4]$ in CH_2Cl_2), thus being difficult to be accurately measured, but which can be tentatively assigned to the Cu(I)/Cu(0) redox couple of the product of the first reduction.

No oxidation processes were observed for these complexes within the potential range covered. However, as a consequence of the reduction process, an oxidation wave around 1.09 V and 1.22 V *vs.* SHE was observed for **1** and **2** respectively, albeit clearer in the case of **2** (see Fig. 4), showing the formation of an electroactive species generated upon a chemical reaction following the above mentioned reduction. It can also be

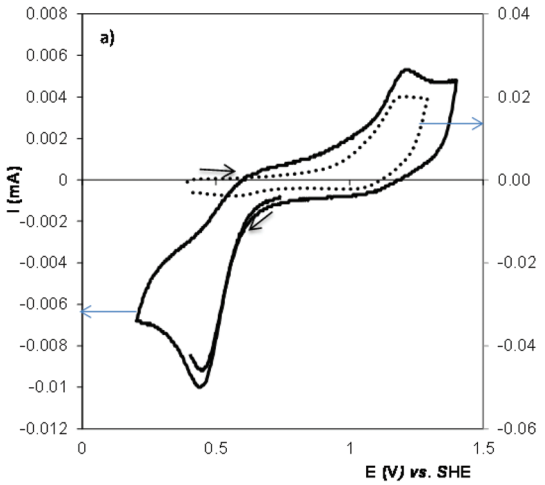

Fig. 4 Cyclic voltammograms of **2** (solid line) and **3** (dotted line) in CH_2Cl_2 at a Pt working electrode. Potentials measured *vs.* SHE at a scan rate of 200 mV s^{-1}.

observed that the chemical reaction is slower for **1** than in the case of **2**, because a small reversibility for the reduction peak is still observed in the first case. Based on the intensity ratio of the anodic/cathodic peaks, this species can be assigned to a dimer $[CuCl(Ar\text{-}BIAN)]_2$, generated by the dimerisation of [CuCl(Ar-BIAN)] formed upon abstraction of a chloride from the anionic complex $[CuCl_2(Ar\text{-}BIAN)]^-$, whose formation is discussed in the theoretical calculations (see the next section). To check this hypothesis, the redox behaviour of **3** was studied in the same electrolyte solution. This compound exhibits a single irreversible oxidation wave at 1.21 V *vs.* SHE (Fig. 4 or Fig. S7a in ESI†), consistent with the potential measured for the oxidation wave described above, which was observed after the reduction of **2**, at 1.22 V *vs.* SHE.

The potentials for the two redox couples are significantly lower (about 0.6 V for the Cu(II)/Cu(I) and 0.8 V for the Cu(I)/Cu(0)) than those observed previously.[28a] These reported compounds are of the $[Cu(Ar\text{-}BIAN)L_2]BF_4$ type, and differ from the present $[Cu(Ar\text{-}BIAN)Cl_2]$ complexes in their cationic nature and from the fact that two chlorides replace the two acetonitrile or benzonitrile ligands. The shift in potential towards more negative values is expected since the chloride ligand has a significantly stronger net electron-donor character than NCMe or NCPh. There are a number of different ligand parameters that can be used to quantify this net-electron donor

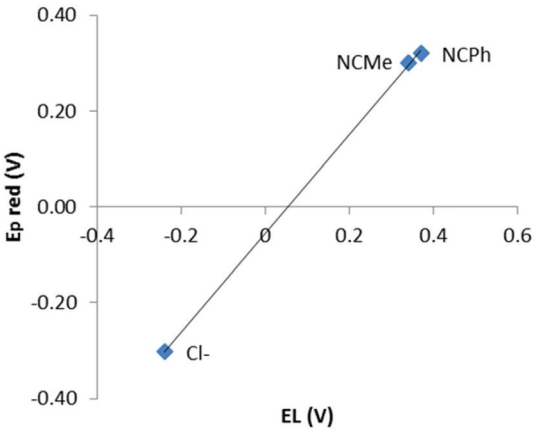

Fig. 5 Reduction peak potentials in CH_2Cl_2 for $[CuCl_2(Ar\text{-}BIAN)]$ (**2**) and $[Cu(Ar\text{-}BIAN)L_2]BF_4$ (where L = NCPh or NCMe)[28a] *vs.* Lever's ligand parameter (EL).

capability of the ligands,[35] such as Pickett's Ligand Parameter (P_L),[36] Lever's parameter (EL)[37] or the more recently proposed $IR_P(L)$.[38] As it can be seen for the case of EL (Fig. 5), the value of the ligand parameter increases with the increase in the potential of the Cu(II)/Cu(I) redox couple.

The fact that the Cu(II)/Cu(I) redox couple is significantly higher in the case of $[Cu(Ar\text{-}BIAN)L_2]BF_4$ complexes than the analogous **1** and **2** shows that they are more stabilised in the Cu(I) oxidation state, as referred in previous work,[28a] in opposition to **1** and **2**, which are more stable in a higher Cu(II) oxidation state.

In MeOH, both complexes **1** and **2** undergo a quasi-reversible reduction process at 200 mV s^{-1}, at E_p^{red} = 0.59 V and E_p^{red} = 0.61 V *vs.* SHE for **1** and **2** respectively, as shown in Table 3 and Fig. S6b in ESI.† Opposite to what was observed in CH_2Cl_2, the formation of the dimeric species upon reduction of **1** or **2** was not detected in this solvent, according to the reversible character of their cathodic processes. The dimer **3** was also studied in MeOH, its redox behaviour consisting of a single quasi-reversible oxidation wave at 0.90 V *vs.* SHE (Fig. S7b in ESI†).

The reduction processes Cu(II)/Cu(I) for **1** and **2** occur in MeOH at higher potentials than in CH_2Cl_2, showing that these complexes are easier to reduce in methanol, in accordance with the theoretical calculations (see the next section). Likewise, the oxidation of the dimer **3** occurs at a higher potential in CH_2Cl_2 than in MeOH, showing that it is easier to oxidise in the latter solvent.

In both solvents the reduction potential is almost unaffected by the substituent on the aryl ring (Mes or Dipp) (Table 3), as expected, taking into account the similarities of the ligands, and in agreement with the results obtained in the theoretical calculations (see the next section).

Since the reduction process seems to be reversible in MeOH, it is reasonable to compare the experimental reduction potential of the redox pair $[CuCl_2(Ar\text{-}BIAN)]/[CuCl_2(Ar\text{-}BIAN)]^-$ with that calculated by DFT and presented in Table 6 (next section). Although the values do not match exactly, the order of magnitude is reasonably comparable, which is probably what would be expected in view of the different approximations both at the experimental and theoretical levels. The values for the potentials in CH_2Cl_2 are quite different since the theoretical calculations indicate that redox potentials should be around 0.3 V lower than those in MeOH, while experimentally we only observe a decrease of around 0.10 V and 0.17 V for **1** and **2**, respectively. However, we note that the difference in the potentials measured *vs.* the internal standard in MeOH and CH_2Cl_2 is much closer to the calculated one (around 0.3 V) and this is partially attributed to the values for the $(Fc^{+/0})$ redox couple in the two solvents, as found in the literature.[39]

(e) Theoretical calculations

We have performed theoretical calculations in order to analyse the different chemical behaviour observed for complexes **1** and **2**. We have evaluated the molecular trends observed for [Cu(II)-(Ar-BIAN)] complexes, the thermodynamics of [Cu(I)(Ar-BIAN)] complexes in solution, and finally performed an estimation of their reduction potentials. This study was carried out with the Ar-BIAN ligand having the following aryl groups: Ph, Mes (*i.e.* complex **1**) and Dipp (*i.e.* complex **2**).

Molecular geometries. The molecular geometry of complexes $[CuCl_2(Ar\text{-}BIAN)]$ (Ar = Ph, Mes, Dipp) has been optimised, their main geometrical parameters are shown in Table 4. In general, bond distances for theoretical and experimental geometries are in agreement, and only a slight lengthening of the Cu–N bonds can be found. In all cases, the Ar-BIAN acts as a bidentate ligand, forming a planar five-membered MN_2C_2 chelate ring. As expected for tetracoordinated

Table 4 Main structural parameters calculated for optimised geometries of $[CuCl_2(Ar\text{-}BIAN)]$ complexes for Ar = Ph, Mes, Dipp, and the corresponding experimental data for complexes **1** and **2**

	Cu–Cl	Cu–N	Cl–Cu–Cl	N–Cu–N	τ^a	ω^a	$S_{SP}{}^b$	$S_{TET}{}^b$
Ph[c]	2.239	2.149	104.1	78.6	129.8	50.8	10.0	10.0
Mes[c]	2.244	2.142	105.0	79.4	103.7	50.2	10.2	9.7
1[d]	2.200	2.048	96.4	81.3	93.3	23.7	2.6	20.9
Dipp[c]	2.252	2.154	98.4	78.7	103.8	29.9	3.4	19.2
2[d]	2.201	2.051	95.7	81.1	92.0	1.5	0.5	33.2

[a] Angles are defined in the text below and in Fig. 6. [b] Continuous shape measures from the ideal square-planar (S_{SP}) or tetrahedral (S_{TET}) geometries. [c] Theoretical values. [d] Experimental values.

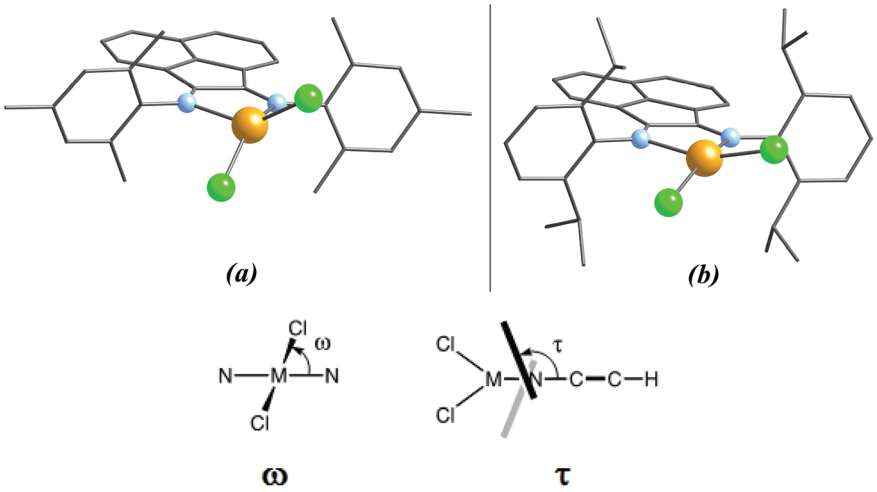

Fig. 6 Views of the optimised geometries of complexes (*a*) [$CuCl_2$(Mes-BIAN)] and (*b*) [$CuCl_2$(Dipp-BIAN)] (top). Definition of the angles ω and τ for structural comparisons (bottom).

Cu(II) centres, the geometry around the metal can be rationalised as square-planar, tetrahedral or intermediate.[40]

To analyse the conformation of [$CuCl_2$(Ar-BIAN)] complexes, we defined the angle ω (Fig. 6, bottom) that measures the relative orientation between the CuN_2 and $CuCl_2$ planes. By definition, for a perfect square-planar coordination ω = 0°, whereas for a tetrahedral one ω = 90°. The optimised geometries for Ph and Mes present values of ω around 50°, and continuous shape measures, S_{SP} and S_{TET} (continuous shape measures quantify deviations from ideal polyhedra[41]), exhibit high values (~10) that do not allow to classify the geometries as square-planar or tetrahedral (the generalised coordinate between both polyhedra determines that the geometry is situated at 52% from the former).[40] The angle ω for Dipp decreases to 30°, and the value of S_{SP} = 3.4 assigns a square-planar coordination to the copper centre. The experimental values are 24 and 2° for complexes **1** and **2**, respectively, and the lowest S_{SP} values are indicative of the square-planar environment in both cases. A clear disagreement between calculated and experimental data is present, but a lower value is always found for the bulkier Dipp aryl group, meaning a geometry closer to square-planar. However, important information can be obtained from a search in the CSD database for *cis*-{$Cu^{II}Cl_2N_2$} cores, revealing that 244 fragments do not present a clear preference for this geometry.

To understand the influence of the angle ω on the behaviour of complexes **1** and **2**, partial optimisations of their structures were performed while varying this angle. The changes in the relative energies are shown in Fig. 7, indicating small energy variations. However, two trends can be distinguished: while relative energy minima of ~2.1 and ~1.7 kcal mol^{-1} were found for $\omega \approx 51°$ and 50° for [$CuCl_2$(Ph-BIAN)] and [$CuCl_2$(Mes-BIAN)] derivatives, respectively, for the complex [$CuCl_2$(Dipp-BIAN)] a dramatic decrease in the relative energy minimum to only 0.16 kcal mol^{-1} is observed for $\omega \approx 30°$ (very close to a perfect square-planar geometry). For the two first

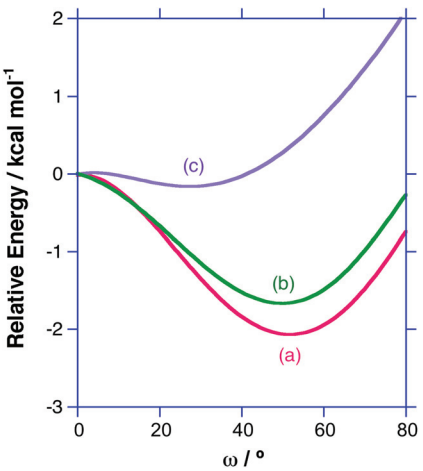

Fig. 7 Relative energy (in kcal mol^{-1}) as a function of angle ω in complexes of the type [$CuCl_2$(Ar-BIAN)] for the cases where aryl groups are: (*a*) Ph, (*b*) Mes, and (*c*) Dipp. Zero values were assigned to the square-planar conformations, ω = 0°.

cases (Ph and Mes), and consistent with the values found experimentally ($\omega \approx 24°$ for **1**), structures with intermediate coordination geometry (between square-planar and tetrahedral) can be anticipated, for which values between 20° and 80° are available in the literature.[40] This is in agreement with the general trends observed, where the square-planar geometry is preferred over the tetrahedral one.[40] This observation also reveals that the methyl groups present in the Mes-ring have only a slight influence on the geometry, whereas the Dipp derivative can only access a square-planar geometry but not a tetrahedral one.

Depending on the molecular geometry of a d^9 ion, the orbital containing the unpaired electron will be located in a $d_{x^2-y^2}$ orbital having the σ-antibonding character (square-planar) or in a less bonding orbital (t_2 orbitals contribute to

the π/σ* character in a tetrahedral complex).[42] Taking into account the influence of the angle ω on the molecular geometry of these complexes, we propose that the complex [$CuCl_2$-(Dipp-BIAN)] is closer to a square-planar environment around the copper centre than [$CuCl_2$(Mes-BIAN)] and, consequently, the reactivity of the former complex can be affected.

Similarly, the angle τ (Fig. 6, bottom) was defined as a measure of the relative orientation of the acenaphthylene backbone in relation to the phenyl rings in the Cu(II) complexes.[23c] In the unsubstituted Ph-BIAN derivative, τ has a value of about 130°, being always larger than 115° when ω is modified.[26a] However, it changes to 103° for *ortho*-substituted aryls that present a CH group (*e.g.* Me = CH_3, iPr = $CH(CH_3)_2$), like in the case of Mes- or Dipp-BIAN, as previously reported.[26a] The analysis of the molecular geometries put in evidence that the presence of short H···Cl distances (3.01 for Me, 2.89 and 3.21 Å for iPr groups) is responsible for the increase of perpendicularity between both groups (for example, $\tau \approx 90°$ when ω is fixed to 0°), as also found in experimental structures.[43]

Reduction to Cu(I). To understand the redox behaviour of the [$CuCl_2$(Ar-BIAN)] complexes, the following possible reduced Cu(I) complexes and their relative stability were considered (Fig. 8, Table 5): (*a*) the anionic [$CuCl_2$(Ar-BIAN)]$^-$, in which an electron was added to the analogous Cu(II) compound, (*b*) [CuCl(Ar-BIAN)], where a chloride was abstracted from the anionic complex, and (*c*) [CuCl(Ar-BIAN)]$_2$, generated by the dimerisation of the latter species. Their relative energies (calculated per copper atom) are shown in Table 5, and coordinates for optimised geometries are available in ESI (Table S3†).

These calculations revealed that the monomeric tetracoordinated [$CuCl_2$(Ar-BIAN)]$^-$ species (Fig. 8 (*a*)) remains always the most stable Cu(I) species, even in dichloromethane and methanol (Table 5). The Cu–N and Cu–Cl distances increase with the reduction from Cu(II) to Cu(I) and the geometry around copper is now tetrahedral, which is the one preferred for a d^{10} ion (the continuous shape measures in our compounds are less than 3.9),[40] with phenyl rings nearly perpendicular to the acenaphthylene backbone.[23c] Similar trends are observed for the angle τ and also for their Cu(II) analogues.[26a] However, a search in the CSD database revealed that no crystal structures having *cis*-{$Cu^ICl_2N_2$}$^-$ cores have been reported to date.

Alternatively, a species such as [CuCl(Ar-BIAN)], in which a chloride anion was removed from the former [$CuCl_2$(Ar-BIAN)]$^-$, can be considered. In this case, the Cu–Cl distance is shorter than that of the related anion, but the remarkable point of the geometry is the asymmetry of the Cu–N bonds, resulting in an intermediate coordination number between three and two.[23c] When considering the {$CuClN_2$} core, the geometry around copper(I) is nearly planar (sum of angles is larger than 356° for all complexes) and a slight bent across N···N is observed (lower than 17°). However, the continuous shape measures show that a linear description ($S_{LIN} < 2.5$) is better than a trigonal one ($S_{TRI} \approx 6$–7). The energy balance is not strongly affected by the nature of the solvent (CH_2Cl_2 or MeOH), and was estimated to be about 7 and 3 kcal mol^{-1} for Mes and Dipp groups, respectively (Table 5). Although the

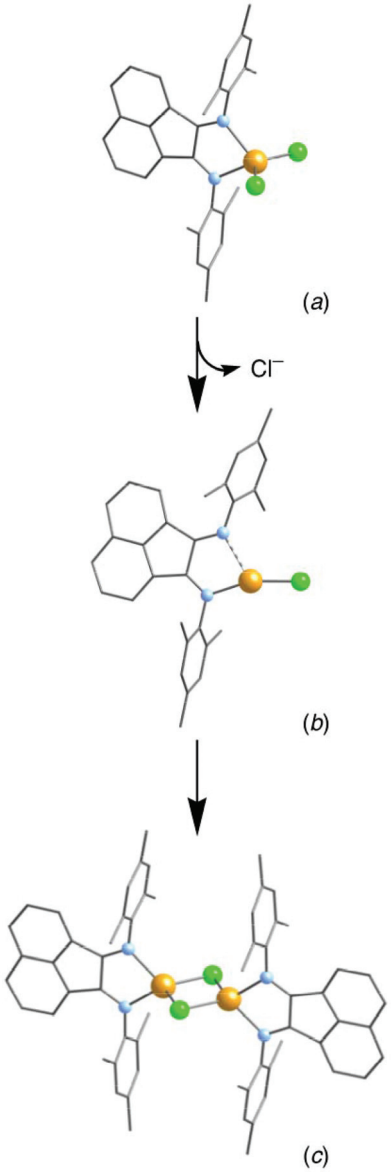

Fig. 8 Molecular structures of Cu(I) complexes: (*a*) [$CuCl_2$(Ar-BIAN)]$^-$, (*b*) [CuCl(Ar-BIAN)], and (*c*) [CuCl(Ar-BIAN)]$_2$.

Table 5 Relative stability per copper (kcal mol^{-1}) for Cu(I) complexes in the gas phase and in CH_2Cl_2 and MeOH solutions. Arbitrary reference is taken from anionic [$CuCl_2$(Ar-BIAN)]$^-$

Ar	Medium	[$CuCl_2$-(Ar-BIAN)]$^-$	[CuCl-(Ar-BIAN)]	1/2 [CuCl-(Ar-BIAN)]$_2$
Ph	Gas phase	0.0	+29.1	+19.8
	CH_2Cl_2	0.0	+8.0	+3.3
	MeOH	0.0	+7.6	+3.2
Mes	Gas phase	0.0	+32.8	+22.0
	CH_2Cl_2	0.0	+7.3	+3.1
	MeOH	0.0	+6.7	+2.8
Dipp	Gas phase	0.0	+32.0	+22.6
	CH_2Cl_2	0.0	+3.7	+1.3
	MeOH	0.0	+3.0	+1.1

change associated with the loss of a chloride is not favoured in both cases, it can be more accessible to the Dipp- than to the Mes-BIAN derivative, as experimentally found. Moreover, our results are in agreement with a higher stability of tetracoordinated copper(I) species in comparison with tricoordinated ones.[44] Despite the fact that 42 entries were found in the CSD database having structurally characterised tricoordinated $\{Cu^{I}ClN_2\}$ cores, we propose that the former $[CuCl_2(Ar\text{-}BIAN)]^-$ complex is a kinetically favoured product, but not a thermodynamically favoured one.

Since the tricoordinated Cu(I) species is coordinatively unsaturated, we analysed the formation of (half) binuclear $[CuCl(Ar\text{-}BIAN)]_2$ having a $\{Cu_2Cl_2\}$ core and a tetrahedral metal centre ($S_{TET} < 4.2$). This unit is planar, with larger Cu–Cl bridging distances, although Cu–N lengths are similar when compared to other compounds. The angles ω determined are larger than 78°, in agreement with the 32 entries found in the CSD (where $\omega > 76°$). Similar trends for the τ angles are observed to that for the mononuclear complexes, and distances between aryl groups are larger than 5.5 Å, discarding any π–π stacking interactions. The low Cu···Cu distances across the diamond could be considered as short, and they were previously analysed by structural and molecular orbital analysis.[45] However, the most important result is the difference of relative energies between the anionic complex $[CuCl_2(Ar\text{-}BIAN)]^-$ and $1/2[CuCl(Ar\text{-}BIAN)]_2$, which was found to be less stable by only ~1 kcal mol^{-1} in the case of the Dipp derivative, whereas it increases to 3 kcal mol^{-1} in the Mes one.

Redox potentials. By simulating the reduction process, we evaluated the redox potentials for Cu(II)/Cu(I) pairs (Table 6). They were estimated from free energies in solution and referenced to the standard hydrogen electrode (SHE). The reference value for methanol is reported by IUPAC, whereas that for dichloromethane had to be deduced, giving less accurate values (see the Computational details section). Consequently, we are aware that values in CH_2Cl_2 have larger uncertainties. At first sight, our calculations revealed an important effect of the solvent in the reduction process, with differences larger than 0.30 V between dichloromethane and methanol. While the influence of the solvent on the redox potential is theoretically overestimated, the trend of the values obtained is however well reproduced. Since the Cu(II)/Cu(I) potential increases clearly from dichloromethane to methanol, Cu(II) complexes become more oxidant in methanol solution, thus facilitating their reduction to Cu(I).

Table 6 Calculated potentials (in V) from SHE for the Cu(II)/Cu(I) reduction pair in dichloromethane and methanol

	$E°$ (V) $[CuCl_2(Ar\text{-}BIAN)]/[CuCl_2(Ar\text{-}BIAN)]^-$		$E°$ (V) $[CuCl_2(Ar\text{-}BIAN)]/[CuCl(Ar\text{-}BIAN)]_2$	
Ar	CH_2Cl_2	MeOH	CH_2Cl_2	MeOH
Mes	0.16	0.47	0.08	0.41
Dipp	0.13	0.44	0.04	0.36

In Table 6 one can notice differences of *ca.* 0.1 V between the $[CuCl_2(Ar\text{-}BIAN)]/[CuCl_2(Ar\text{-}BIAN)]^-$ and $[CuCl_2(Ar\text{-}BIAN)]/[CuCl(Ar\text{-}BIAN)]_2$ pairs in each of the solvents. These differences are caused by the relative stability of Cu(I) complexes. Since the anion $[CuCl_2(Ar\text{-}BIAN)]^-$ is more stable than the binuclear $[CuCl(Ar\text{-}BIAN)]_2$, the participation of the former complex in the couple increases the reduction potential. However, the small differences observed indicate that the reduced species practically has no effect on the electrochemical properties of our systems. Additionally, the influence of the substituents on the aryl ring is negligible (<0.05 V) between Mes and Dipp. These results suggest that the experimental behaviour will be determined by the relative stability of the Cu(I) species together with the solvent effect.

(f) Metal-mediated radical polymerisation

Both complexes **1** and **2** have been tested in metal-mediated radical polymerisation of styrene under reverse-ATRP conditions. The experiments were carried out using the conventional 2,2′-azobisisobutyronitrile (AIBN) free radical initiator, which is one of the safer and less expensive commercial initiators.

In a preliminary reaction, complexes **1** and **2** were compared under the same reaction conditions, *i.e.* [styrene]/[Cu]/[AIBN] = 200/1/0.8, in toluene (50% v/v), at 80 °C. After 45 h reaction, the complex **1** yielded 81% of polystyrene with a M_n value slightly higher than the expected one ($M_{n(GPC)}$ = 22 900 g mol^{-1}, $M_{n(Theo)}$ = 16 872 g mol^{-1}, PDI = 2.32). The latter sample of polystyrene was studied by ^1H and ^{13}C NMR (Fig. S8–S10 in ESI†), and a triad sequence analysis was performed, revealing a microstructure typical of a completely atactic polymer: mm = 0.16, mr = 0.69 and rr = 0.15; P_m = 0.50. The complex **2** was found to be less active (67% conversion after 48 h), and did not lead to a better controlled polymerization reaction, as determined by the mass properties of the final polymer ($M_{n(GPC)}$ = 26 000 g mol^{-1}, $M_{n(Theo)}$ = 13 956 g mol^{-1}, PDI = 2.15). This fact and the tendency of the Cu^{II} compound **2** to be reduced to the dimeric Cu^{I} complex **3** in air constrained us to focus our investigations on the controlled character of the polymerisation reaction only for the complex **1**.

A clearly linear first-order kinetic plot obtained in the polymerisation reaction mediated by the complex **1** (Fig. 9, and Table S1 in ESI†) indicates a constant radical concentration in solution, in agreement with the reverse-ATRP mechanism. The controlled character of the polymerisation process is highlighted by the linear increase of the number-average molecular weight (M_n) and a nearly constant polydispersity index (PDI = 2.2–2.4) (Fig. 10 and Table S1 in ESI†). The experimental M_n of the polystyrene produced is slightly higher than the theoretical one (Fig. 10). An attempt to better control the polystyrene M_n by running the reaction in a more diluted medium (styrene–toluene 1 : 3) was unsuccessful.

In summary, using the common radical initiator AIBN, the air-stable Cu^{II} complex **1** containing the ligand (2,4,6-

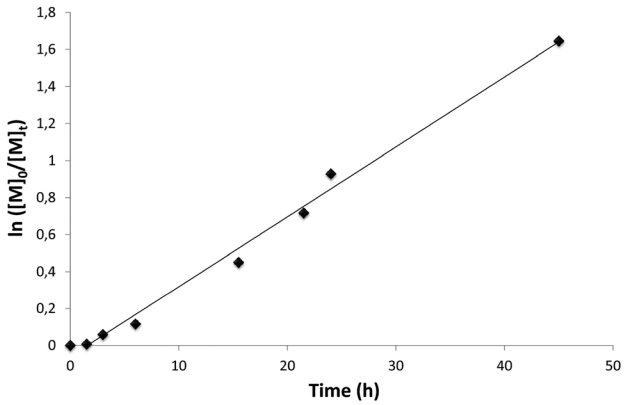

Fig. 9 First-order kinetic plot for the reverse-ATRP of styrene using the complex **1**. Conditions: [styrene]/[Cu]/[AIBN] = 200/1/0.8, toluene (50% v/v), 80 °C.

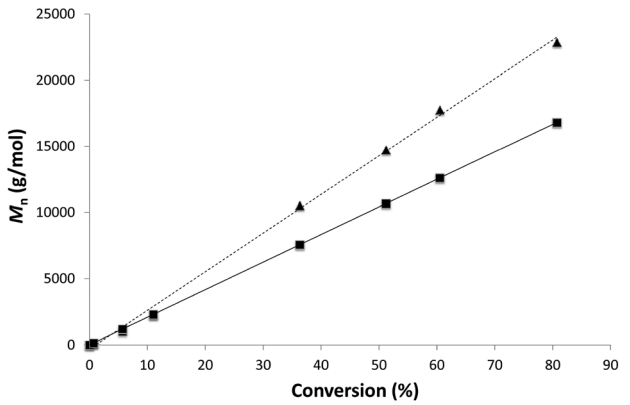

Fig. 10 Experimental (triangles and dashed line) and theoretical (squares and plain line) dependence of M_n of the synthesized polystyrene on monomer conversion (%). Conditions: [styrene]/[Cu]/[AIBN] = 200/1/0.8, toluene (50% v/v), 80 °C.

$Me_3C_6H_2$)-BIAN was found to mediate the polymerisation of styrene in a controlled manner, under mild conditions.

Conclusions

Two new Ar-BIAN Cu(II) complexes [$CuCl_2$(Mes-BIAN)] (**1**) and [$CuCl_2$(Dipp-BIAN)] (**2**) were synthesised and fully characterised by several techniques including X-ray crystallography. Their solid-state molecular structures showed different geometries around the copper atom. Density functional theory calculations showed that oxidised copper(II) complexes favour intermediate geometries between square-planar and tetrahedral, but the bulkier isopropyl groups, in agreement with the experimental results, favour the former geometry, whereas reduced copper(I) prefers the tetrahedral environment. The determination of the reduction potentials by cyclic voltammetry allowed us to identify the influence of dichloromethane and methanol solvents, explaining the different experimental behaviours observed for compounds **1** and **2** in methanol, which was corroborated by the DFT calculations. The complex **1** was found to mediate the polymerisation of styrene in a controlled manner, under mild conditions, using the common radical initiator AIBN (under reverse-ATRP conditions).

Experimental

General procedures and materials

All reactions and manipulations of solutions were performed under an argon atmosphere using Schlenk techniques, except where stated. Solvents were of reagent grade and were dried according to literature methods, distilled and stored under argon. Ligands **L1** and **L2** were prepared according to the literature.[16]

Elemental analyses were performed at the Analytical Services of the Laboratory of REQUIMTE-Departamento de Química, Universidade Nova de Lisboa, on a Thermo Finnigan-CE Flash-EA 1112-CHNS instrument. Infrared spectra were recorded in the region 4000–100 cm^{-1} on a Nicolet 6700 FT-IR spectrometer (ATR mode, SMART ORBIT accessory, Diamond crystal). Gas chromatography (GC) analyses were performed on a KoniK HRGC 4000 B using a DB-Wax column (30 m, 0.25 mm ID, 0.25 μm Film).

Gel permeation chromatography (GPC/SEC) analyses were performed at 35 °C on a Shimadzu LC20AD ultra-fast liquid chromatograph equipped with a Shimadzu RID10A refractometer detector. A Varian PLgel pre-column and two Varian PLgel 5 μm MIXED-C columns were used in series. HPLC-grade THF was used as the eluent, at a flow rate of 1.0 mL min^{-1}. Calibrations were performed using polystyrene standards (400–100 000 g mol^{-1}).

The AIBN solution (0.2 M in toluene) and styrene were purchased from Sigma-Aldrich. Styrene was dried over CaH_2, distilled and stored under argon before use.

Syntheses of complexes

Method A. The following procedure was adopted: a suspension of $CuCl_2$ in CH_2Cl_2 (5 mL) was treated with the corresponding solution of the Ar-BIAN ligand in CH_2Cl_2 (25 mL). The mixture was left stirring for 12 h, at room temperature. After reaction, the solution was filtered, concentrated and pentane or diethyl ether was added to precipitate crystals of the desired product without the need for further purification.

Complex 1: Ligand **L1** (0.5 g, 1.2 mmol), $CuCl_2$ (0.162 g, 1.2 mmol). Complex **1**, 0.61 g, yield: 92%. Brown crystals were obtained by slow diffusion of diethyl ether in a dichloromethane solution of **1**.

Elemental analysis calcd (%) for $C_{30}H_{28}Cl_2CuN_2 \cdot 1/2CH_2Cl_2$: C 61.73, H 4.93, N 4.72; found: C 61.76, H 5.41, N 4.23.

FTIR ν (cm^{-1}): 1660 (C═N), 1638 (C═N); Far-IR ν (cm^{-1}): 524, 357, 323.

^{1}H NMR (400 MHz, CD_2Cl_2): δ 17.68, 14.39, 12.25, 9.35, 6.98, 6.30, 5.35, 5.11, 2.35, 2.29, 1.75, 1.59, 1.45, 1.39, 1.37, 1.24, 0.97.

MALDI-TOF-MS: m/z = 401.21 $[\mathbf{L1} - CH_3]^+$; 514.11 $[\mathbf{L1}CuCl]^+$.

Complex 2: Ligand **L2** (0.5 g, 1 mmol), $CuCl_2$ (0.134 g, 1 mmol). Complex **2**, 0.55 g, yield: 87%. Dark green needles were obtained by slow diffusion of pentane in a dichloromethane solution of **2**.

Elemental analysis calcd (%) for $C_{36}H_{40}Cl_2CuN_2$: C 68.07, H 6.35, N 4.41; found: C 68.05, H 6.37, N 4.37.

FTIR ν (cm^{-1}): 1666 (C═N), 1636 (C═N); Far-IR ν (cm^{-1}): 526, 355, 321.

^1H NMR (400 MHz, CD_2Cl_2): δ 14.49, 10.43, 5.97, 5.40, 3.21, 2.14, 1.57, 1.30, 0.92.

MALDI-TOF-MS: m/z = 457.24 $[\mathbf{L2} - iPr]^+$; 598.19 $[\mathbf{L2}CuCl]^+$.

Method B. The following procedure was adopted: a green solution of $CuCl_2$ (0.080 g, 0.6 mmol) in MeOH (5 mL) was added dropwise to an orange solution of the equimolar amount of Ar-BIAN ligand in CH_2Cl_2 (15 mL). In both reactions there was a colour change to brown (with **L1**) or to dark green (with **L2**). The mixture was left under stirring for 2 h and subsequently filtered. The filtrate was left standing at room temperature, in air, for evaporation. After 48 h, brown crystals of **1** (reaction of **L1** with $CuCl_2$), or black crystals of **3** (reaction of **L2** with $CuCl_2$) formed. The crystals were separated and characterised by single crystal X-ray diffraction. While in the case of **1** the yield was high (90%) and no side products were formed, in the case of **3** yellow crystals of uncharacterised side-products also formed, the yield of **3** being lower (45%).

Mass spectrometry

MALDI-TOF-MS (Matrix Assisted Laser Desorption Ionization-Time of Flight-Mass Spectrometry) analysis were performed at the REQUIMTE-MALDI-TOF-MS Service Laboratory, and have been performed in a MALDI-TOF-MS Voyager DE-PRO Biospectrometry Workstation equipped with a nitrogen laser radiating at 337 nm from Applied Biosystems (Foster City, USA). MALDI mass spectra were acquired and treated with the Data Explorer software version 4 series. The MALDI-TOF-MS study in dichloromethane was carried out for all the synthesised compounds. Samples were dissolved in dichloromethane (1 μg μL^{-1}), and 1 to 2 μL of the corresponding solution was spotted on a well of a MALDI-TOF-MS sample plate and allowed to dry. No matrix was added. Measurements were performed in the reflector positive or negative ion mode, with a 20 kV accelerating voltage, 80% grid voltage, 0.005% guide wire, and a delay time of 200 ns. Mass spectral analysis for each sample was based on the average of 500 laser shots.

NMR measurements

Nuclear Magnetic Resonance (NMR) spectra of complexes **1** and **2**, and of polystyrenes were acquired using Bruker Avance III 400 MHz (^1H, 400.132 MHz; ^{13}C, 100.623 MHz) spectrometers, equipped with a 5 mm BBO inverse detection probe and a 5 mm BBO detection probe, respectively, and variable temperature control units.

Exact quantities of polycrystalline samples of complexes **1** and **2** (*cf.* Table 2) were dissolved in 500 μL of a mixture of the deuterated dichloromethane solvent and a small amount of tetramethylsilane (TMS). The same mixture was added to a capillary insert, co-axial with the NMR tube. The ^1H NMR spectra were acquired with a spectral window of 200 ppm centred around 6.175 ppm (to observe any potentially shifted peaks by the paramagnetic Cu ion), and their frequencies were calibrated using the TMS resonance of the capillary tube. All spectra were acquired at 298 K. Mass magnetic susceptibility measurements were performed using the Evans method.[46] The number of free electrons was calculated using the approximations described in ref. 47.

The ^1H and $^{13}C\{^1H\}$ NMR spectra of the polystyrenes, in 1,1,2,2-tetrachloroethane-d_2 solutions, were run at 120 °C. Spectra were referenced internally using the residual protio or the ^{13}C solvent resonances relative to TMS (δ = 0). All chemical shifts are quoted in δ (ppm). The measurement of observed intensities of triad sequences was performed by electronic integration within the range of the *ipso* carbon $^{13}C\{^1H\}$ NMR resonance (see Fig. S9 in ESI†), the corresponding values being normalised. The isotactic reaction probability (P_m)[48] was calculated according to the equation P_m = mm + 1/2mr, in which mm and mr are the normalised intensities of the corresponding triads.

EPR measurements

X-band CW-EPR spectra of polycrystalline samples were recorded at 77 K and 298 K with a Bruker EMX spectrometer using a rectangular cavity with 100 kHz field modulation, and equipped with an Oxford continuous flow cryostat. Powder samples were obtained by grinding single-crystals. Solutions were prepared dissolving this powder in CH_2Cl_2. All sample manipulations were performed under an argon atmosphere in a glovebox with a dioxygen concentration below 1 ppm. EPR parameters of powdered and solution samples were obtained from spectral simulations using the software Simfonia (v. 1.25, Bruker Instruments Inc.).

X-ray data collection, structure solution and refinement

Suitable crystals for the X-ray analysis of **1**·OEt_2, **2**·CH_2Cl_2 and **3** were obtained as described in the Experimental section. The intensity data were collected on a Kappa CCD diffractometer[49] (graphite monochromated MoKα radiation, λ = 0.71073 Å) at 173(2) K. Crystallographic and experimental details for the structures are summarised in Table 7. The structures were solved by direct methods (SHELXS-97) and refined by full-matrix least-squares procedures (based on F^2, SHELXL-97)[50] with anisotropic thermal parameters for all the non-hydrogen atoms, except for those of the diethyl ether molecule co-crystallised with compound **1**. The crystal **1** showed the presence of a disordered diethyl ether molecule, for which some restraints to distances and angles were applied and the non-hydrogen atoms being refined with isotropic thermal parameters. The CH_2Cl_2 solvent molecule in **2**·CH_2Cl_2 was found severely disordered and since attempts to identify the atomic positions failed, a PLATON-SQUEEZE[51] procedure was applied. The residual electron density was assigned to one molecule of

Table 7 Crystallographic data for complexes **1**·OEt_2, **2**·CH_2Cl_2 and **3**

Compound reference	**1**·OEt_2	**2**·CH_2Cl_2	**3**
Chemical formula	$C_{30}H_{28}Cl_2CuN_2{\cdot}C_4H_{10}O$	$C_{36}H_{40}Cl_2CuN_2{\cdot}CH_2Cl_2$	$C_{72}H_{80}Cl_2Cu_2N_4$
Formula mass	625.10	720.07	1199.38
Crystal system	Orthorhombic	Monoclinic	Monoclinic
a/Å	17.015(3)	11.7040(4)	16.2640(11)
b/Å	16.611(4)	29.0320(10)	12.2230(10)
c/Å	22.891(6)	11.9346(4)	22.2710(10)
α/°	90.00	90.00	90.00
β/°	90.00	105.32(3)	132.99(5)
γ/°	90.00	90.00	90.00
Unit cell volume/Å^3	6470(3)	3911.1(6)	3238(3)
Temperature/K	173(2)	173(2)	173(2)
Space group	*Pbca*	$P2_1/c$	$P2_1/c$
Z	8	4	2
Absorption coefficient, μ/mm^{-1}	0.868	0.857	0.783
No. of reflections measured	43 539	31 167	21 322
No. of independent reflections	9445	10 407	9426
R_{int}	0.0884	0.0315	0.0864
R_1 values ($I > 2\sigma(I)$)	0.0809	0.0698	0.0646
w$R(F^2)$ values ($I > 2\sigma(I)$)	0.2144	0.1581	0.1683
R_1 values (all data)	0.1350	0.0965	0.1014
w$R(F^2)$ values (all data)	0.2390	0.1686	0.1995
S on F^2	1.094	1.057	1.051

dichloromethane. This data treatment resulted in an improved quality of the model. The hydrogen atoms were introduced into the geometrically calculated positions (SHELXS-97 procedures) and refined riding on the corresponding parent atoms, with C–H distances of 0.95, 0.98, 0.99 and 1.00 Å for aromatic, methyl, methylene, and methine H atoms, respectively, and with $U_{iso}(H) = 1.2U_{eq}(C)$. CCDC 994399–994401 contain the supplementary crystallographic data.

Electrochemical measurements

Cyclic voltammetry experiments were performed using a Radiometer DEA 101 Digital Electrochemical Analyser interfaced with an IMT 102 Electrochemical Interface. The cell was a 5 mL three-electrode cell equipped with a Pt disc (1 mm radius) working electrode, a Pt-wire auxiliary electrode and a Ag-wire pseudo-reference electrode, kept in a separate compartment and connected to the main compartment by a Luggin capillary. The potentials were measured with a scan rate of 200 mV s^{-1} against an internal standard, the ferrocenium/ferrocene ($Fc^{+/0}$) couple, according to the IUPAC recommendations.[52] In order to compare these experimental potentials with the theoretical potentials they were converted to the Ag/AgCl/KCl (sat.) reference electrode scale according to the reduction potentials published for the $Fc^{+/0}$ couple in methanol and dichloromethane, 418 mV and 520 mV, respectively,[39] and then to the Standard Hydrogen Electrode (SHE) scale using the value of 222 mV for the Ag/AgCl reference electrode *versus* SHE.[53] Solutions of $[NBu_4][BF_4]$ in CH_2Cl_2 or MeOH (0.2 M) were used as electrolytes, the concentrations of complexes being in the range 1.2–1.3 mM. All experiments were carried out in the absence of oxygen. Dry nitrogen was bubbled through the solution in the cell before each scan.

Computational details

Unrestricted calculations were carried out using the Gaussian09 package.[54] The hybrid density functional method known as B3LYP was applied.[55] Effective core potentials (ECP) were used to represent the innermost electrons of the transition atoms and the basis set of valence double-ζ quality associated with the pseudopotentials known as LANL2DZ.[56] The basis set for the light elements such as C, N and H was 6-31G*.[57] Energies in solution were taken into account by PCM calculations (dichloromethane and methanol, ε = 8.93 and 32.613, respectively),[58] maintaining the geometry optimised for the gas phase (single-point calculations). Reduction potentials are estimated from free energies in these solvents, taking 4.32 and 4.19 V as references for the absolute SHE in dichloromethane and methanol, respectively. The latter value is given in the IUPAC recommendations,[59] whereas the former has been obtained from solvent effects introduced in the ferrocene/ferrocenium pair.[60]

Structural analysis

The structural data were obtained through a systematic search in the Cambridge Structural Database (version 5.33 with two updates, February 2012).[61] Shape continuous measures were calculated with the SHAPE program,[62] which provides quantitative information of how much the environment deviates from an ideal polyhedron, helping the assignment of the geometry of the coordination sphere around the metal.

General procedure for the styrene polymerisation experiments

The solid catalyst (0.5 mol%, 20 mg, 36.30 μmol) was placed in a pre-dried Schlenk tube equipped with a stirring bar and three vacuum/argon cycles were performed. Then styrene (200 equiv., 834.5 μL, 7.26 mmol), toluene (834.5 μL) and the AIBN solution (0.8 equiv., 145.2 μL, 29.04 μmol) were added *via* a

syringe. The solution was degassed by three freeze–pump–thaw cycles and a reference sample was collected. The Schlenk tube was then immersed in an oil bath at 80 °C and aliquots were removed at different reaction times, diluted in THF, filtered through neutral alumina and analysed by gas chromatography (GC) in order to determine the reaction conversion. For isolation of the polymer, the reaction mixture was precipitated in cold methanol, filtered, washed with additional methanol, and dried under vacuum. The polystyrene samples obtained were then analysed by GPC/SEC.

Acknowledgements

We thank *Fundação para a Ciência e Tecnologia* (FCT), Portugal, for funding (projects PTDC/QUI-QUI/099873/2008, PEst-C/EQB/LA0006/2013, PTDC/EQU-EQU/110313/2009, PEst-OE/QUI/UI0100/2013) and for fellowships SFRH/BPD/73253/2010 (C.F.), SFRH/BPD/44262/2008 (V.R.), SFRH/BPD/80293/2011 (R.M.A.) and SFRH/BPD/64423/2009 (C.S.B.G.). P.J.G. thanks Programa Ciência 2008. The authors acknowledge LabRMN at FCT-UNL and *Rede Nacional de RMN* (RNRMN) for access to the facilities. *Rede Nacional de RMN* is supported with funds from FCT, Projecto de Re-Equipamento Científico, Portugal. We also thank for financial support the *Spanish Dirección General de Investigación*, *Desarrollo e Innovación* (*MINECO*) through grant CTQ2011-23862-C01 and the *Departament d'Economia i Coneixement* of *Generalitat de Catalunya* through grant 2009SGR-1459. The computing resources at the *Centre de Supercomputació de Catalunya* (CESCA) were made available in part through a grant of *Fundació Catalana per a la Recerca* (FCR) and *Universitat de Barcelona*.

References

1 P. J. Pérez and M. M. Díaz-Requejo, in *Comprehensive Organometallic Chemistry III*, ed. R. H. Crabtree and D. M. P. Mingos, Elsevier, New York, 2007, vol. 2, pp. 153–195.
2 Recently, in 2012, the entire issue no. 22 (volume no. 31) of *Organometallics* was fully dedicated to organocopper chemistry: *Organometallics*, 2012, **31**, 7631–8038.
3 J.-S. Wang and K. Matyjaszewski, *J. Am. Chem. Soc.*, 1995, **117**, 5614.
4 M. Kato, M. Kamigaito, M. Sawamoto and T. Higashimura, *Macromolecules*, 1995, **28**, 1721.
5 T. E. Patten and K. Matyjaszewski, *Acc. Chem. Res.*, 1999, **32**, 895.
6 K. Matyjaszewski and J. H. Xia, *Chem. Rev.*, 2001, **101**, 2921.
7 T. Pintauer and K. Matyjaszewski, *Chem. Soc. Rev.*, 2008, **37**, 1087.
8 M. Ouchi, T. Terashima and M. Sawamoto, *Chem. Rev.*, 2009, **109**, 4963.
9 F. Di Lena and K. Matyjaszewski, *Prog. Polym. Sci.*, 2010, **35**, 959.
10 T. Pintauer and K. Matyjaszewski, *Coord. Chem. Rev.*, 2005, **249**, 1155.
11 S. Gulli, J.-C. Daran and R. Poli, *Eur. J. Inorg. Chem.*, 2011, 1666.
12 Y. Champouret, S. Gulli, J.-C. Daran and R. Poli, *Eur. J. Inorg. Chem.*, 2012, 1672.
13 (*a*) M. Dvolaitzky, *C. R. Acad. Sci. Paris, Ser. C*, 1969, **268**, 1811; (*b*) M. Dvolaitzky, *Chem. Abstr.*, 1969, **71**, 61566b.
14 (*a*) I. Matei and T. Lixandru, *Bull. Ist. Politeh. Iasi*, 1967, **13**, 245; (*b*) I. Matei and T. Lixandru, *Chem. Abstr.*, 1969, **70**, 3623m.
15 (*a*) H. Tom Dieck, M. Svoboda and T. Greiser, *Z. Naturforsch., B: Anorg. Chem. Org. Chem.*, 1981, **36**, 823; (*b*) G. van Koten and K. Vrieze, *Adv. Organomet. Chem.*, 1982, **21**, 151, and references cited therein.
16 R. van Asselt, C. J. Elsevier, J. J. W. Smeets, A. L. Spek and R. Benedix, *Recl. Trav. Chim. Pays-Bas*, 1994, **113**, 88.
17 B. Rieger, L. Saunders Baugh, S. Kacker and S. Striegler, *Late Transition Metal Polymerization Catalysis*, Wiley-VCH, Weinheim, 2003.
18 (*a*) S. D. Ittel, L. K. Johnson and M. Brookhart, *Chem. Rev.*, 2000, **100**, 1169; (*b*) G. J. P. Britovsek, V. C. Gibson and D. F. Wass, *Angew. Chem., Int. Ed.*, 1999, **38**, 429; (*c*) V. C. Gibson and S. K. Spitzmesser, *Chem. Rev.*, 2003, **103**, 283.
19 J. H. Groen, J. G. P. Delis, P. W. N. M. van Leeuwen and K. Vrieze, *Organometallics*, 1997, **16**, 68.
20 J. Durand and B. Milani, *Coord. Chem. Rev.*, 2006, **250**, 542.
21 A. Scarel, M. R. Axet, F. Amoroso, F. Ragaini, C. J. Elsevier, A. Holuigue, C. Carfagna, L. Mosca and B. Milani, *Organometallics*, 2008, **27**, 1486.
22 B. L. Small, R. Rios, E. R. Fernandez and M. J. Carney, *Organometallics*, 2007, **26**, 1744.
23 (*a*) V. Rosa, P. J. Gonzalez, T. Avilés, P. T. Gomes, R. Welter, A. C. Rizzi, M. C. G. Passeggi and C. D. Brondino, *Eur. J. Inorg. Chem.*, 2006, 4761; (*b*) V. Rosa, S. A. Carabineiro, T. Avilés, P. T. Gomes, R. Welter, J. M. Campos and M. R. Ribeiro, *J. Organomet. Chem.*, 2008, **693**, 769; (*c*) V. Rosa, T. Avilés, G. Aullón, B. Covelo and C. Lodeiro, *Inorg. Chem.*, 2008, **47**, 7734.
24 L. Li, C. S. B. Gomes, P. T. Gomes, M. T. Duarte and Z. Fan, *Dalton Trans.*, 2011, **40**, 3365.
25 C. Romain, V. Rosa, C. Fliedel, F. Bier, F. Hild, R. Welter, S. Dagorne and T. Avilés, *Dalton Trans.*, 2012, **41**, 3377.
26 (*a*) V. Rosa, C. I. M. Santos, R. Welter, G. Aullón, C. Lodeiro and T. Avilés, *Inorg. Chem.*, 2010, **49**, 8699; (*b*) T. Kern, U. Monkowius, M. Zabel and G. Knör, *Eur. J. Inorg. Chem.*, 2010, 4148.
27 (*a*) U. El-Ayaan, F. Murata, S. El-Derby and Y. Fukuda, *J. Mol. Struct.*, 2004, **692**, 209; (*b*) A. Paulovicova, U. El-Ayaan, K. Shibayama, T. Morita and Y. Fukuda, *Eur. J. Inorg. Chem.*, 2001, 2641.
28 (*a*) L. Li, P. S. Lopes, V. Rosa, C. A. Figueira, M. A. N. D. A. Lemos, M. T. Duarte, T. Avilés and P. T. Gomes, *Dalton Trans.*, 2012, **41**, 5144; (*b*) L. Li, P. S. Lopes, C. A. Figueira, C. S. B. Gomes, M. T. Duarte,

V. Rosa, C. Fliedel, T. Avilés and P. T. Gomes, *Eur. J. Inorg. Chem.*, 2013, 1404.

29 See for instance: (*a*) P. Chaudhuri, M. Hess, J. Müller, K. Hildenbrand, E. Bill, T. Weyhermuller and K. Wieghardt, *J. Am. Chem. Soc.*, 1999, **121**, 9599; (*b*) S. E. Balaghi, E. Safaei, L. Chiang, E. W. Y. Wong, D. Savard, R. M. Clarkeb and T. Storr, *Dalton Trans.*, 2013, **42**, 6829.

30 T. Kern, U. Monkowius, M. Zabel and G. Knör, *Inorg. Chim. Acta*, 2011, **374**, 632.

31 (*a*) L. E. Karagiannidis, P. A. Gale, M. E. Light, M. Massi and M. I. Ogden, *Dalton Trans.*, 2011, **40**, 12097; (*b*) M. J. Spallek, S. Stockinger, R. Goddard, F. Rominger and O. Trapp, *Eur. J. Inorg. Chem.*, 2011, 5014; (*c*) P. Drabina, P. Valenta, P. Jansa, A. Růžička, J. Hanusek and M. Sedlák, *Polyhedron*, 2008, **27**, 268; (*d*) V. C. Gibson, A. Tomov, D. F. Wass, A. J. P. White and D. J. Williams, *J. Chem. Soc., Dalton Trans.*, 2002, 2261.

32 (*a*) F. Sączewski, E. Dziemidowicz-Borys, P. J. Bednarski, R. Grünert, M. Gdaniec and P. Tabin, *J. Inorg. Biochem.*, 2006, **100**, 1389; (*b*) S. F. Haddad and J. Pickardt, *Transition Met. Chem.*, 1993, **18**, 377.

33 (*a*) M. Mégnamisi-Bélombé, P. Singh, D. E. Bolster and W. E. Hatfield, *Inorg. Chem.*, 1984, **23**, 2578; (*b*) M. Mégnamisi-Bélombé and H. Enders, *Acta Crystallogr., Sect. C: Cryst. Struct. Commun.*, 1983, **39**, 707; (*c*) M. Mégnamisi-Bélombé and M. A. Novotny, *Inorg. Chem.*, 1980, **19**, 2470.

34 H. T. Dieck and L. Stamp, *Acta Crystallogr., Sect. C: Cryst. Struct. Commun.*, 1983, **39**, 841.

35 L. Perrin, E. Clot, O. Eisenstein, J. Loch and R. H. Crabtree, *Inorg. Chem.*, 2001, **40**, 5806.

36 J. Chatt, C. T. Kan, G. J. Leigh, C. J. Pickett and D. R. Stanley, *J. Chem. Soc., Dalton Trans.*, 1980, 2032.

37 A. B. P. Lever, *Inorg. Chem.*, 1990, **29**, 1271.

38 F. Zobi, *Inorg. Chem.*, 2009, **48**, 10845.

39 I. Noviandri, K. N. Brown, D. S. Fleming, P. T. Gulyas, P. A. Lay, A. F. Masters and L. Phillips, *J. Phys. Chem. B*, 1999, **103**, 6713.

40 J. Cirera, P. Alemany and S. Alvarez, *Chem. – Eur. J.*, 2004, **10**, 190.

41 S. Alvarez, P. Alemany, D. Casanova, J. Cirera, M. Llunell and D. Avnir, *Coord. Chem. Rev.*, 2005, **249**, 1693.

42 S. Alvarez, A. A. Palacios and G. Aullón, *Coord. Chem. Rev.*, 1999, **185–186**, 431.

43 G. Aullón, D. Bellamy, L. Brammer, E. A. Bruton and A. G. Orpen, *Chem. Commun.*, 1998, 653.

44 M. A. Carvajal, J. J. Novoa and S. Alvarez, *J. Am. Chem. Soc.*, 2004, **126**, 1465.

45 P. Alemany and S. Alvarez, *Inorg. Chem.*, 1992, **31**, 4266.

46 D. F. Evans, *J. Chem. Soc.*, 1959, 2003.

47 (*a*) G. Pass and H. Sutcliffe, *J. Chem. Educ.*, 1971, **48**, 180; (*b*) J. L. Deutsch and S. M. Poling, *J. Chem. Educ.*, 1969, **46**, 167.

48 (*a*) F. A. Bovey, *High Resolution NMR of Macromolecules*, Academic Press, New York, 1st edn, 1972, pp. 146–181; (*b*) L. Li, C. S. B. Gomes, P. S. Lopes, P. T. Gomes, H. P. Diogo and J. R. Ascenso, *Eur. Polym. J.*, 2011, **47**, 1636, and references cited therein; (*c*) L. C. Silva, P. T. Gomes, L. F. Veiros, S. I. Pascu, M. T. Duarte, S. Namorado, J. R. Ascenso and A. R. Dias, *Organometallics*, 2006, **25**, 4391.

49 Bruker-Nonius, *Kappa CCD Reference Manual*, Nonius BV, The Netherlands, 1998.

50 G. M. Sheldrick, *Acta Crystallogr., Sect. A: Fundam. Crystallogr.*, 2008, **64**, 112.

51 A. L. Spek, *J. Appl. Crystallogr.*, 2003, **36**, 7.

52 G. Gritzner and J. Kuta, *Electrochim. Acta*, 1984, **29**, 869.

53 R. G. Bates and J. B. Macaskill, *Pure Appl. Chem.*, 1978, **50**, 1701.

54 M. J. Frisch, G. W. Trucks, H. B. Schlegel, G. E. Scuseria, M. A. Robb, J. R. Cheeseman, G. Scalmani, V. Barone, B. Mennucci, G. A. Petersson, H. Nakatsuji, M. Caricato, X. Li, H. P. Hratchian, A. F. Izmaylov, J. Bloino, G. Zheng, J. L. Sonnenberg, M. Hada, M. Ehara, K. Toyota, R. Fukuda, J. Hasegawa, M. Ishida, T. Nakajima, Y. Honda, O. Kitao, H. Nakai, T. Vreven, J. A. Montgomery Jr., J. E. Peralta, F. Ogliaro, M. Bearpark, J. J. Heyd, E. Brothers, K. N. Kudin, V. N. Staroverov, T. Keith, R. Kobayashi, J. Normand, K. Raghavachari, A. Rendell, J. C. Burant, S. S. Iyengar, J. Tomasi, M. Cossi, N. Rega, J. M. Millam, M. Klene, J. E. Knox, J. B. Cross, V. Bakken, C. Adamo, J. Jaramillo, R. Gomperts, R. E. Stratmann, O. Yazyev, A. J. Austin, R. Cammi, C. Pomelli, J. W. Ochterski, R. L. Martin, K. Morokuma, V. G. Zakrzewski, G. A. Voth, P. Salvador, J. J. Dannenberg, S. Dapprich, A. D. Daniels, O. Farkas, J. B. Foresman, J. V. Ortiz, J. Cioslowski and D. J. Fox, *Gaussian 09 (Revision B.1)*, Gaussian Inc., Wallingford, CT, 2010.

55 (*a*) A. D. Becke, *J. Chem. Phys.*, 1993, **98**, 5648; (*b*) C. Lee, W. Yang and R. G. Parr, *Phys. Rev. B: Condens. Matter*, 1988, **37**, 785.

56 P. J. Hay and W. R. Wadt, *J. Chem. Phys.*, 1985, **82**, 299.

57 (*a*) P. C. Hariharan and J. A. Pople, *Theor. Chim. Acta*, 1973, **28**, 213; (*b*) M. M. Francl, W. J. Petro, W. J. Hehre, J. S. Binkley, M. S. Gordon, D. J. DeFrees and J. A. Pople, *J. Chem. Phys.*, 1982, **77**, 3654.

58 (*a*) J. Tomasi and M. Persico, *Chem. Rev.*, 1994, **94**, 2027; (*b*) C. Amovilla, V. Barone, R. Cammi, E. Cancès, M. Cossi, B. Mennucci, C. S. Pomelli and J. Tomasi, *Adv. Quantum Chem.*, 1998, **32**, 227.

59 (*a*) S. Trasatti, *Pure Appl. Chem.*, 1986, **58**, 955; (*b*) I. Persson, *Pure Appl. Chem.*, 1986, **58**, 1153.

60 P. Zanello, *Inorganic Electrochemistry*, RSC, Cambridge, 1st edn, 2003, pp. 589–594.

61 F. H. Allen and O. Kennard, *Chem. Des. Autom. News*, 1993, **8**, 31.

62 M. Llunell, D. Casanova, J. Cirera, P. Alemany and S. Alvarez, *SHAPE (version 2.0)*, Barcelona, 2010.

